Anti-Inflammatory Dinuclear Copper(II) Complexes with Indomethacin. Synthesis, Magnetism and EPR Spectroscopy. Crystal Structure of the *N*,*N*-Dimethylformamide Adduct

Jane E. Weder,[†] Trevor W. Hambley,*[,†] Brendan J. Kennedy,*[,†] Peter A. Lay,*[,†] Dugald MacLachlan,[†,‡] Richard Bramley,[§] Christopher D. Delfs,[§] Keith S. Murray,[||] Boujemaa Moubaraki,[||] Barry Warwick,[⊥] John R. Biffin,[⊥] and Hubertus L. Regtop[⊥]

School of Chemistry, University of Sydney, Sydney, NSW 2006, Australia, Research School of Chemistry, Australian National University, Canberra, ACT 0200, Australia, Department of Chemistry, Monash University, Melbourne, VIC 3168, Australia, and Biochemical Veterinary Research Pty. Ltd., Braemar, NSW 2575, Australia

Received September 11, 1998

Veterinary anti-inflammatory Cu(II) complexes of indomethacin (1-(4-chlorobenzoyl)-5-methoxy-2-methyl-1*H*-indole-3-acetic acid = IndoH), of the general formula $[Cu_2(Indo)_4L_2]$ (L = *N*,*N*-dimethylformamide (DMF), *N*,*N*-dimethylacetamide (DMA), *N*-methylpyrrolidone (NMP), and water), were studied by zero-field and X-band EPR spectroscopies, electronic spectroscopy, magnetic measurements, and X-ray powder diffraction. The complexes are similar to Cu(II) acetate monohydrate, with a strong antiferromagnetic exchange interaction, *J*, ranging from -141 to -152 cm^{-1}. Variable temperature magnetic susceptibility data for all of the complexes are similar, with the exception of a $[Cu_2(Indo)_4(H_2O)_2]$ complex, which displays an unusual increase in magnetic moment with decreasing temperature from 50 to 10 K. The X-ray powder diffraction patterns of the DMF and DMA dimers show that they are isostructural. Two isostructural H_2O complexes were synthesized from different methods yet displayed different variable temperature magnetic susceptibity data. All of the $[Cu_2(Indo)_4L_2]$ complexes crystallize in the triclinic space group $P\bar{1}$. Single-crystal X-ray diffraction analysis of the DMF complex, $[Cu_2(Indo)_4(DMF)_2]\cdot 1.6(DMF)$, shows that it is similar to the previously reported $[Cu_2(Indo)_4(DMSO)_2]$ with a Cu−Cu bond length of 2.630(1) Å, Cu−O_{RCOO} of 1.960(4)−1.967(4) Å, and Cu−O_{DMF} of 2.143(5) Å and crystal parameters a = 10.848(3) Å, b = 13.336(6) Å, c = 16.457(4) Å, α = 104.67(3)°, β = 100.94(2)°, and γ = 107.16(3)°. The X-ray structure of the DMF dimer does not exhibit strong intermolecular interactions due to the hydrophobic nature of the exterior. This may be important in facilitating its dissolution in micelles and transport through membranes.

Introduction

Over the past 30 years, numerous reports have appeared on the benefits of Cu(I) and Cu(II) compounds in the treatment of inflammation.[1−5] A range of Cu complexes have been studied as anti-inflammatory agents, ranging from simple Cu salts[6,7] to monomeric and dimeric Cu(II)−carboxylato complexes.[8] In addition, Cu(II) complexes of clinically used nonsteroidal anti-inflammatory drugs (NSAIDs) are often more potent anti-inflammatory agents than either the parent NSAID drug or the uncomplexed Cu salt.[3,8] Furthermore, there are suggestions that Cu may play a role in preventing the gastrointestinal damage associated with use of the NSAIDs.[3,9]

The mechanism of the analgesic and anti-inflammatory action of the NSAIDs is still a matter of some debate;[10,11] however, these compounds have been shown to be potent inhibitors of prostaglandin synthesis.[10,12−14] Indomethacin (**I**) is one of the most potent of the clinically used NSAIDs[15] and interferes with prostaglandin synthesis by direct inhibition of the two cyclooxygenase enzyme systems, Cox-1 and Cox-2.[16,17] Inhibition of the Cox-2 system results in anti-inflammatory action, while inhibition of the Cox-1 enzyme system results in anti-inflammatory

[†] University of Sydney.
[‡] Current address: National Registration Authority for Agricultural and Veterinary Chemicals, PO Box E240, Kingston, ACT 2604, Australia.
[§] Australian National University.
[||] Monash University.
[⊥] Biochemical Veterinary Research Pty. Ltd.

(1) Bonta, I. L. *Acta Physiol. Pharmacol. Neerl.* **1969**, *15*, 188−222.
(2) Adams, S. S.; Cobb, R. *Prog. Med. Chem.* **1976**, *5*, 59−138.
(3) Sorenson, J. R. J. *Inflammatory Diseases and Copper*, 1st ed.; Humana Press: Clifton, NJ, 1982.
(4) Sorenson, J. R. J.; Kishore, V.; Pezeshk, A.; Oberley, L. W.; Leuthauser, S. W. C. *Inorg. Chim. Acta* **1984**, *91*, 285−294.
(5) Sorenson, J. R. J. *A Physiological Basis for Pharmacological Activities of Copper Complexes: An Hypothesis*; Humana Press: Clifton, NJ, 1987; pp 3−16.
(6) Sorenson, J. R. J. *J. Med. Chem.* **1976**, *19*, 135−148.
(7) Lewis, A. J. *Agents Actions* **1978**, *8*, 244−250.
(8) Sorenson, J. R. J. *Prog. Med. Chem.* **1989**, *26*, 437−568.
(9) Boyle, E.; Freeman, P. C.; Goudie, A. C.; Mangan, F. R.; Thomson, M. *J. Pharm. Pharmacal.* **1976**, *28*, 865−868.
(10) Abramson, S. B.; Weissmann, G. *Arthritis Rheum.* **1989**, *32*, 1−9.
(11) Thomas, J. *Australian Presciption Products Guide*, 26th ed.; Australian Pharmaceutical Publishing Co. Ltd.: Hawthorn, Victoria, 1997; Vol. 1, pp 1327−1336.
(12) Vane, J. R. *NATUA* **1971**, *231*, 232−235.
(13) Vane, J. R.; Ferreira, S. H. *Anti-inflammatory Drugs*; Springer-Verlag: New York, 1979.
(14) Moncada, S.; Vane, J. R. *Adv. Intern. Med.* **1979**, *24*, 1−22.
(15) Dukes, M. N. G. *Meyler's Side Effects of Drugs, An Encyclopedia of Adverse Reactions and Interactions*, 13th ed.; Elsevier: Amsterdam, 1996.
(16) Ouellet, M.; Percival, M. D. *J. Biochem.* **1995**, *306*, 247−251.
(17) Vane, J. R.; Botting, R. M. *Semin. Arthritis Rheum.* **1997**, *26*, 2−10.

10.1021/ic981100x CCC: $18.00
Published on Web 03/31/1999

action as well as gastric irritation.[15,18] Gastrointestinal irritation and ulceration are recognized as significant side effects of NSAIDs.[11,19,20]

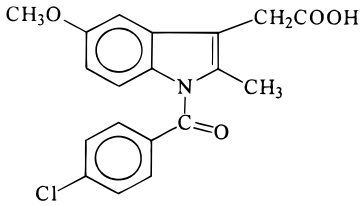

I

Interest in developing potent yet less irritating NSAIDs has led to several studies on the preparation, characterization, and veterinary and medical use of divalent metal salts of IndoH and a number of other NSAIDs.[3,21−25] Carboxylate-type NSAIDs produce dinuclear ($[Cu^{II}_2(RCOO)_4L_2]$) and mononuclear ($[Cu^{II}(RCOO)_2L_2]$) complexes, where R = aryl or phenyl group, and L has included a variety of ligands such as water, caffeine, imidazole, diethylamine, 3-picoline, *N*,*N*-dimethylformamide, dimethyl sulfoxide, 3-pyridylmethanol, and pyridine.[22,23,25−31]

The characterization of Cu(II) complexes of IndoH is important because of their increasing use as veterinary pharmaceutics and their potential for use as potent human anti-inflammatory drugs. Here we report on the synthesis, the electronic, zero-field EPR, and X-band EPR spectroscopies, the magnetic properties, and the X-ray powder and crystal diffraction characteristics of Cu(II)−Indo and its solvent adducts with DMF, DMA, NMP, and water. These studies are important to establish the structures of the active components of the pharmaceutical preparations.

Experimental Section

Synthesis. All of the complexes are green crystalline or powdered solids soluble in DMF, tetrahydrofuran (THF), and acetonitrile and insoluble in water. IndoH was of pharmaceutical grade (Sigma Pharmaceuticals). All of the other chemicals were of analytical grade (Aldrich or Sigma) and were used without further purification.

Bis(*N*,*N*′-dimethylformamide)tetrakis-μ-(*O*,*O*′-Indo)dicopper(II) *N*,*N*′-Dimethylformamide Dihydrate, $[Cu_2(Indo)_4(DMF)_2]\cdot DMF\cdot 2H_2O$. To a warm (∼50 °C) DMF (20 mL) solution of IndoH (14.3 g, 0.04 mol) was added a solution of Cu(II) acetate monohydrate (4 g, 0.02 mol) in DMF (25 mL), and the mixture was heated to 80 °C. Ethanol (250 mL) was added to the mixture with vigorous shaking, and the resulting deep green solution was set aside for about 1 day, during which time the Cu complex separated as a microcrystalline light green powder. The mixture was filtered under vacuum, and the green product was washed exhaustively with ethanol (100 mL) and dried overnight at room temperature. Yield: 13.9 g (76%). Anal. ($Cu_2C_{85}H_{85}Cl_4N_7O_{21}$) C, H, N, Cu: calcd, 56.42, 4.73, 5.42, 7.02; found, 56.41, 4.55, 5.41, 7.05.

Bis(*N*,*N*′-dimethylformamide)tetrakis-μ-(*O*,*O*′-Indo)dicopper(II) 1.6-*N*,*N*′-Dimethylformamide, $[Cu_2(Indo)_4(DMF)_2]\cdot 1.6(DMF)$. The complex was crystallized from a 36% w/v solution of $[Cu_2(Indo)_4(DMF)_2]$ dissolved in a mixture of 20% DMF and 80% ethanol. Anal. ($Cu_2C_{86.8}H_{85.2}Cl_4N_{7.6}O_{19.6}$) C, H, N: calcd, 57.4, 4.7, 5.9; found, 57.8, 4.8, 5.9.

Bis(*N*,*N*′-dimethylacetamide)tetrakis-μ-(*O*,*O*′-Indo)dicopper(II) Trihydrate, $[Cu_2(Indo)_4(DMA)_2]\cdot 3H_2O$. The complex was prepared in a manner similar to that for $[Cu_2(Indo)_4(DMF)_2]$, except that *N*,*N*-dimethylacetamide was used as the solvent. Ethanol was added, and the solution was cooled overnight to yield a microcrystalline dark green precipitate. The mixture was filtered under vacuum and the product was washed exhaustively with ethanol (150−300 mL), dried overnight at room temperature, and finally dried at 40 °C for 8 h. Yield: 6.40 g (35%). Anal. ($Cu_2C_{84}H_{84}Cl_4N_6O_{21}$) C, H, N, Cu: calcd, 56.60, 4.75, 4.72, 7.13; found, 56.16, 4.94, 4.86, 7.52.

Diaquatetrakis-μ-(*O*,*O*′-Indo)dicopper(II) sesquihydrate, $[Cu_2(Indo)_4(OH_2)_2]\cdot 1.5H_2O$. IndoH (4 g, 0.01 mol) in ethanol (50 mL) was added to Cu(II) acetate monohydrate (1 g, 0.005 mol) in ethanol (50 mL), and a pale green Cu complex began to precipitate within minutes of mixing. While the resultant solution was being shaken vigorously, ethanol (150 mL) was added: then the mixture was left to stand at room temperature overnight. The mixture was filtered under vacuum and dried overnight at room temperature. Yield: 3.9 g (78%). Anal. ($Cu_2C_{76}H_{69}Cl_4N_4O_{20.5}$) C, H, N, Cu: calcd, 56.44, 4.18, 3.46, 7.86; found, 56.30, 4.26. 3.62, 8.10.

Diaquatetrakis-μ-(*O*,*O*′-Indo)dicopper(II), $[Cu_2(Indo)_4(H_2O)_2]$. To a sodium hydroxide solution (0.1 M, 100 mL) was added IndoH (14.3, 0.04 mol), and the resulting solution was filtered to remove undissolved IndoH. Copper(II) chloride dihydrate (1 g, 0.006 mol) in water (25 mL) was added and the solution was heated to 50 °C, during which time the Cu complex separated as a pale green powder. The mixture was filtered under vacuum, and the green product was washed exhaustively with ethanol and water. Yield: 11.9 g (78%). Anal. ($Cu_2C_{76}H_{64}Cl_4N_4O_{18}$) C, H, N, Cu: calcd, 57.40, 4.06, 3.52, 7.99; found, 57.65. 4.06, 3.98, 7.90.

Bis(*N*-methyl-2-pyrrolidone)tetrakis-μ-(*O*,*O*′-Indo)dicopper(II) Dihydrate, $[Cu_2(Indo)_4(NMP)_2]\cdot 2H_2O$. The *N*-methylpyrrolidone complex was prepared by the method described for $[Cu_2(Indo)_4(DMF)_2]$ except that *N*-methylpyrrolidone was used as the solvent. Yield: 12.08 g (66%). Anal. ($Cu_2C_{86}H_{82}Cl_4N_6O_{20}$) C, H, N, Cu: calcd, 57.75, 4.62, 4.70, 7.11; found: 57.76, 4.54, 4.76, 7.85.

Physical Measurements. Metal analyses were determined using a Varian AA-800 air−acetylene flame atomic absorption spectrophotometer. The C, H, N elemental analyses of the powdered samples were performed by the Department of Chemical Engineering, University of Sydney. The C, H, N elemental analysis of the $[Cu_2(Indo)_4(DMF)_2]\cdot$1.6(DMF) crystal was performed by the National Analytical Laboratories (NAL).

Room temperature magnetic moments (μ_{eff}) were measured on a Sherwood Scientific magnetic susceptibility balance. Variable temperature magnetic data were collected in the range 5−300 K using a Quantum Design MPMS SQUID magnetometer. The samples were cooled in zero field. In all cases the raw data were corrected for the diamagnetic sample holder. The strength of the antiferromagnetic coupling constant, *J*, defined as

$$H_{ex} = -2J\hat{\mathbf{S}}_1\cdot\hat{\mathbf{S}}_2 \qquad (1)$$

(18) Fenner, H. *Semin. Arthritis Rheum.* **1997**, *26*, 28−33.
(19) Goodman, L. S.; Gilman, A. *The Pharmacological Basis of Therapeutics*, 5th ed.; Macmillan Publishing Co., Inc.: New York, 1975.
(20) Reynolds, J. E. F. *Martindale. The Extra Pharmacopoeia*, 13th ed.; The Pharmaceutical Press: London, 1993.
(21) Auer, D. E. Copper, Inflammation and Copper Containing Anti-inflammatory Drugs in the Horse. Ph.D. Thesis, University of Queensland, Brisbane, 1987; pp 1−273.
(22) Abuhijleh, A. L.; Bogas, E.; Le Guenniou, G. *Inorg. Chim. Acta* **1992**, *195*, 67−71.
(23) Abuhijleh, A. L. *J. Inorg. Biochem.* **1994**, *55*, 255−262.
(24) Dendrinou-Samara, C.; Kessissoglou, D. P.; Manoussakis, G. E.; Mentzafos, D.; Terzis, A. *J. Chem. Soc., Dalton Trans.* **1990**, 959−965.
(25) Dendrinou-Samara, C.; Jannakoudakis, P. D.; Kessissoglou, D. P.; Manoussakis, G. E.; Mentzafos, D.; Terzis, A. *J. Chem. Soc., Dalton Trans.* **1992**, 3259−3264.
(26) Regtop, H. L.; Biffin, J. R. Preparation of Divalent Metal Salts of Indomethacin. US Patent 5310936; Biochemical Veterinary Research Pty. Ltd., Australia, 1994.
(27) Underhill, A. E.; Bougourd, S. A.; Flugge, M. L.; Gale, S. E.; Gomm, P. S. *J. Inorg. Biochem.* **1993**, *52*, 139−144.
(28) Bhirud, R. G.; Srivastave, T. S. *Inorg. Chim. Acta* **1990**, *173*, 121−125.
(29) Valach, F.; Tokarcik, M.; Kubinex, P.; Melnik, M.; Macaskova, L. *Polyhedron* **1997**, *16*, 1461−1464.
(30) Melnik, M.; Potocnak, I.; Macaskova, L.; Miklos, D.; Holloway, C. E. *Polyhedron* **1996**, *15*, 2159−2164.
(31) Reimann, G. W.; Kokoszka, G. F.; Gordon, G. *Inorg. Chem.* **1965**, *4*, 1082−1084.

was obtained by fitting the data to the Bleaney−Bowers equation,[32]

$$\chi_A = \frac{N\beta^2\bar{g}^2}{3kT}(1-x)\left[\frac{3\exp(-2J/kT)}{3\exp(-2J/kT)+1}\right] + N_\alpha + \frac{4x}{T} \qquad (2)$$

where $\bar{g}$ is the average g value for the dimer, χ_A represents the magnetic susceptibility per Cu, x is the fraction of monomer, β is the Bohr magneton, N is the Avogadro constant, and N_α is a temperature independent contribution to the susceptibility. In the fitting procedure, all of the experimentally observed susceptibilities were equally weighted and final fits were obtained by minimizing the function in eq 3.

$$E = \sum[(\chi_{obsd} - \chi_{calcd})T]^2 \qquad (3)$$

Solid state IR (400−2000 cm^{-1}) and far-IR (75−500 cm^{-1}) spectra were acquired in pressed disks of KBr and polyethylene, respectively, on a Bruker IFS 66v FTIR spectrophotometer at a resolution of 1.0 cm^{-1}.

Diffuse reflectance solid state and solution (DMF) UV−vis electronic spectra were recorded from 200 to 1200 nm and 400−900 nm, respectively, using a Varian Cary 5E UV−vis−near-IR spectrophotometer. Spectra of the solid samples of the complexes were acquired in a KBr matrix. The spectra of the DMF solutions were acquired in 1-cm quartz cells in the double-beam acquisition mode.

Zero-field EPR spectra (ZFEPR) of powdered samples were recorded using a resonant reflection zero-field EPR spectrometer similar to that described elsewhere.[33−35] The zero-field splitting parameters, D, E, and $A_{||}$, were obtained from eq 4,[33,35]

$$H_S = D(S_z^2 - S(S+1)/3) + E(S_x^2 - S_y^2) + A_{||}S_zI_z \qquad (4)$$

with the axial direction being along the Cu−Cu vector. As the perpendicular hyperfine constituents were unresolved, they are not included in the equation. In the analysis it was assumed that the antiferromagnetic coupling of the two Cu(II) sites was sufficiently strong that the singlet−triplet separation was significantly greater than D.

Low-temperature X-band powder EPR spectra of the solid $[Cu_2(Indo)_2L_2]$ samples were measured at X-band frequencies (∼9.5 GHz) using a Bruker EMX EPR spectrometer equipped with a standard ER4120 X-band cavity, gaussmeter, frequency counter, BVT2000 variable temperature unit, and Oxford Instruments E900 continuous flow cryostat. The values of $g_{||}$ and $g_\perp$ were determined from the resulting X-band spectra using the values of D and E obtained from the ZFEPR studies. The powder EPR spectra are described by the spin Hamiltonian,

$$H = \beta BgS + D(S_x^2 - 2\beta) + E(S_x^2 - S_y^2) \qquad (5)$$

where B, the external magnetic field, g, the anisotropic Lande splitting tensor, S, the total spin vector, and D and E, the zero-field splitting parameters, were derived directly from the observed zero-field EPR spectrum. The values of g were obtained using the EPRPOW and SIMER simulation programs.[36,37]

Powder X-ray diffraction patterns were collected at room temperature using Cu Kα radiation on a SIEMENS D5000 diffractometer with divergence and antiscatter slits of 1 mm, and receiver and detector slits of 0.2 and 0.6 mm, respectively. The data were collected over the range 2.0−35.0° in steps of 0.04° in 2θ, and a count time per step of 15.0 s.

The X-ray crystallographic data for $[Cu_2(Indo)_4(DMF)_2]\cdot 1.6(DMF)$ were measured on an Enraf-Nonius CAD4F four-circle diffractometer employing graphite-monochromated Mo Kα radiation. Lattice parameters at 21 °C were determined by a least-squares fit to the setting parameters of 25 independent reflections.

Intensity data were collected in the range $1° < \theta < 21°$ using an $\omega - 0.67\theta$ scan. The scan widths and horizontal counter apertures employed were $(1.30 + 0.35 \tan\theta)°$ and $(2.30 + 0.5 \tan\theta)$ mm. Data reduction and application of Lorentz, polarization, and decomposition (6.4%) corrections were carried out using the Enraf-Nonius Structure Determination Package.[38] Absorption corrections were not applied. Of the 4572 independent nonzero reflections collected, 2744 with $I > 2.5\sigma(I)$ were considered observed and used in the calculations.

The structure was solved by direct methods using SHELXS-76,[39] and the solution was extended by difference Fourier methods. Hydrogen atoms were included at calculated sites (C−H 0.97 Å) with group isotropic thermal parameters, and all other atoms, with the exception of minor contributors to disordered species (DMF molecules), were refined anistropically. Blocked-matrix least-squares refinements of an overall scale factor and positional and thermal parameters converged with all shifts $<0.4\,\sigma$. Maximum excursions in a final difference map were +0.33 and −0.25 e $Å^{-3}$. Scattering factors and anomalous dispersion terms used for Cu (neutral Cu) were taken from *International Tables for X-Ray Crystallography*,[40] and all others used were those supplied by SHELX-76.[39] All calculations were carried out using SHELX-76,[39] and plots were drawn using ORTEP.[41]

Solution Stability. The stability of $[Cu_2(Indo)_4(DMF)_2]$ in aqueous micelle solutions of the biological buffers HEPES (*N*-2-hydroxyethylpiperazine-*N*′-2-ethanesulfonic acid) and TES (*N*-tris(hydroxymethyl)methyl-2-aminoethanesulfonic acid) was determined by dissolving ∼1−2 mg mL^{-1} of the complex in 100 mM buffer with 40 mM sodium dodecyl sulfate (SDS) in Milli-Q water adjusted to *p*H ∼7.4 and measuring the EPR and UV−vis spectra of the resulting solutions. In addition, the stability of $[Cu_2(Indo)_4(DMF)_2]$ in an aqueous veterinary manufacturing solution comprising 48 mg mL^{-1} of the complex dissolved in micelles of Span 80 plus tetraglycol was also determined. The % Cu(II) monomer concentrations were calculated by determining the double integral of the Cu(II) monomer spectra of the unknown samples and comparing to a $CuCl_2$ calibration curve. Glycerin 20% was added to the biological buffer and $CuCl_2$ calibration samples to produce vitrified samples suitable for EPR spectroscopy. The UV−vis and EPR spectra of the $[Cu_2(Indo)_4(DMF)_2]$ HEPES and TES buffers were measured over a period of 3 days.

Results

Syntheses. The complexes $[Cu_2(Indo)_4(OH_2)_2]\cdot 1.5H_2O$ and $[Cu_2(Indo)_4L_2]$ (L = DMF, DMA, NMP) were prepared by heating a 2:1 molar ratio of IndoH and Cu(II) acetate monohydrate (or 6.7:1 molar ratio of IndoH/Cu(II) chloride dihydrate for $[Cu_2(Indo)_4(OH_2)_2]$) in the appropriate solvent. The dimer was precipitated by the addition of excess ethanol. A dimeric species was also prepared using MeCN as the solvent, but on precipitation with EtOH, microanalysis demonstrated that the resulting complex was the water adduct, $[Cu_2(Indo)_4(OH_2)_2]$.

Crystal Structure of the $[Cu_2(Indo)_4(DMF)_2]\cdot 1.6(DMF)$ Complex. The crystal data and data collection parameters for $[Cu_2(Indo)_4(DMF)_2]\cdot 1.6(DMF)$ are given in Table 1 and selected bond lengths and angles in Table 2. The atomic numbering system and ORTEP diagram are given in Figures 1 and 2, respectively. Tables of non-hydrogen coordinates and isotropic thermal parameters, bond distances, bond angles, anisotropic thermal parameters, hydrogen atom positions, and isotropic thermal parameters for $[Cu_2(Indo)_4(DMF)_2]\cdot 1.6(DMF)$ and a

(32) Bleaney, B.; Bowers, K. *Proc. R. Soc. London, Ser. A* **1952**, 451−465.
(33) Delfs, C. D.; Bramley, R. *Chem. Phys. Lett.* **1997**, *264*, 333−337.
(34) Delfs, C. D.; Bramley, R. *J. Chem. Phys.* **1997**, *107*, 8840−8847.
(35) Bramley, R.; Strach, S. *Chem. Rev.* **1983**, *83*, 49−82.
(36) MacLachlan, D. *EPRPOW Computer Program for Simulation of EPR Spectra*; University of Sydney: Sydney, 1996.
(37) MacLachlan, D. *SIMER Computer Program for Rapid Simulation of EPR Spectra*; University of Sydney: Sydney, 1996.
(38) *Enraf-Nonius Structure Determination Package*; Enraf-Nonius: Delft, Holland, 1985.
(39) Sheldrick, G. M. *SHELX-76: A Program for X-ray Crystal Structure Determination*; University of Cambridge: Cambridge, 1976.
(40) Cromer, D. T.; Waber, J. T. *International Tables for X-Ray Crystallography*; The Kynoch Press: Birmingham, England, 1974; Vol. 4.
(41) Johnson, C. K. *ORTEP. A Thermal Ellipsoid Plotting Program*; Oak Ridge National Laboratories: Oak Ridge, TN, 1976.

Table 1. Crystal and Data Collection Parameters for $[Cu_2(Indo)_4(DMF)_2]\cdot 1.6(DMF)$

formula	$Cu_2C_{86.8}H_{85.2}Cl_4N_{7.6}O_{19.6}$
M_r	1817.2
cryst color	green
cryst dimens (mm)	0.10 × 0.15 × 0.15
cryst syst	triclinic
space group	$P\bar{1}$
a (Å)	10.848(3)
b (Å)	13.336(6)
c (Å)	16.457(4)
α (deg)	104.67(3)
β (deg)	100.94(2)
γ (deg)	107.16(3)
V (Å^3)	2109(2)
Z	1
D_{calc} (g cm^{-3})	1.437
radiation (monochromated incident beam) λ(Mo Kα) (Å)	0.7107
μ(Mo Kα) (cm^{-1})	6.88
$R1$[a]	0.046
wR2[b]	0.048

[a] $R1 = \sum(||F_o| - |F_c||)/\sum|F_o|$. [b] $wR2 = \sum(w^{1/2}||F_o| - |F_c||)/\sum w^{1/2}|F_o|$, $w = 0.75/(\sigma^2(F_o) + 0.0010F_o^2)$.

Table 2. Selected Interatomic Distances (Å) and Angles (deg) in $[Cu_2(Indo)_4(DMF)_2]\cdot 1.6(DMF)$[a]

Cu_1-Cu_1*	2.630(1)	Cu_1*$-O_5$	1.967(4)
$Cu-O_1$	1.960(4)	Cu_1-O_6	1.963(5)
Cu_1*$-O_2$	1.947(4)	Cu_1-O_9	2.143(5)
$O_6-Cu_1-O_1$	88.9(2)	Cu_1*$-O_2-C_1$	124.5(5)
$O_9-Cu_1-O_1$	93.9(2)	$O_6-Cu_1-Cu_1$*	84.2(1)
$O_9-Cu_1-O_6$	94.5(2)	O_5*$-Cu_1-Cu_1$*	84.1(1)
$Cu_1-O_6-C_{21}$	122.5(5)	$O_6-Cu_1-O_2$*	89.1(2)
$O_9-Cu_1-O_5$*	97.2(2)	O_2*$-Cu_1-O_5$*	89.8(2)
$C_{21}-O_5-Cu_1$*	122.4(5)	O_5*$-Cu_1-O_1$	89.8(2)
$Cu_1-O_1-C_1$	123.2(5)	$O_6-C_{21}-O_5$	126.9(7)
$O_1-C_1-O_2$	123.9(6)		

[a] Atoms are labeled as depicted in Figure 1. Asterisks (*) depict atom labeling assuming an inverted point of symmetry centered midway along the Cu−Cu vector. Standard deviations, in parentheses, occur in the last significant figure.

figure presenting the atomic numbering system for Indo in the crystal structure of $[Cu_2(Indo)_4(DMF)_2]\cdot 1.6(DMF)$ are given in the Supporting Information.

The structure consists of two Cu atoms linked by four Indo groups in a fashion similar to that of $[Cu_2(Indo)_4(DMSO)_2]$[42] and the dinuclear structure of $[Cu_2(CH_3COO)_4(H_2O)_2]$.[43−46] A DMF molecule is bound trans to the Cu−Cu vector on each of the Cu atoms, and a further two DMF molecules are loosely held in the lattice. These lattice DMF sites were highly mobile, and their sites were only partially occupied. During the data collection, some reductions in the intensities of the standard reflections were noted, and these are consistent with slow loss of these molecules of crystallization. The fused and conjugated five- and six-membered rings are close to being coplanar (deviations less than 0.04 Å), and the Cu dimer makes no close contacts with other molecules in the lattice. The structure of

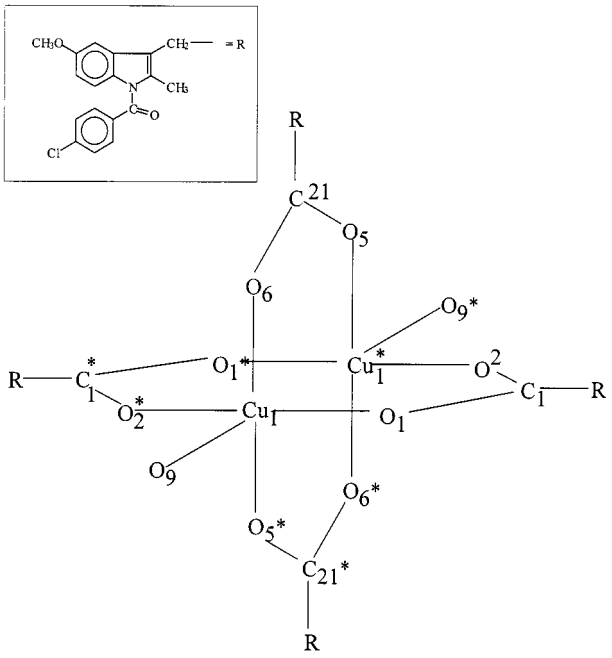

Figure 1. Atomic numbering system for the complex in the crystal structure of $[Cu_2(Indo)_4(DMF)_2]\cdot 1.6DMF$.

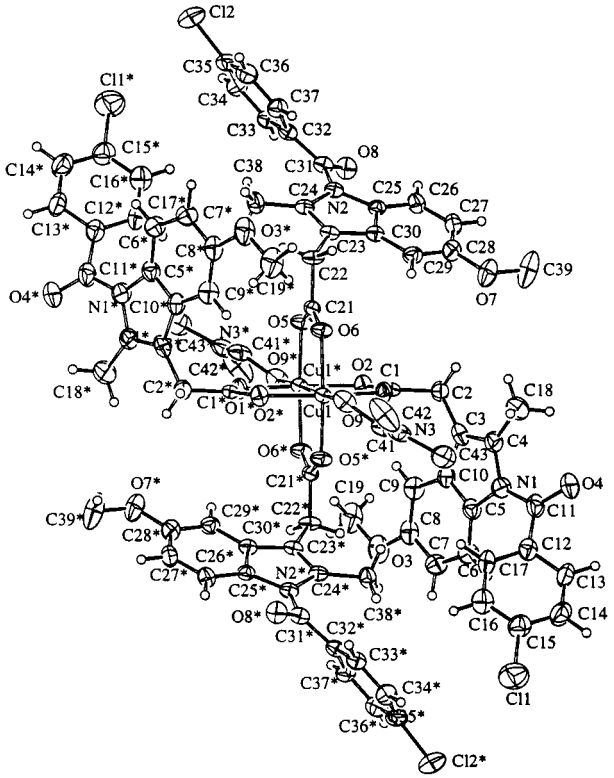

Figure 2. ORTEP diagram of the complex in the crystal structure of $[Cu_2(Indo)_4(DMF)_2]\cdot 1.6$ DMF.

the $[Cu_2(Indo)_4(DMF)_2]\cdot 1.6(DMF)$ complex is similar to that reported for the DMSO complex,[42] although the latter structure was of a much lower precision.

The individual Cu atoms have a Jahn−Teller-distorted, octahedral geometry, with four short $Cu-O_{RCOO}$ (1.960(4)−1.967(4) Å) bond lengths and a long solvent Cu−O (2.143(5) Å) bond length. The two copper atoms in each dimeric unit are separated by a distance of 2.630(1) Å. This distance is similar to that found in $[Cu_2(Indo)_4(DMSO)_2]$[42] (2.632(6) Å) and other

(42) Weser, U.; Sellinger, K. H.; Lengfelder, E.; Werner, W.; Strahle, J. *Biochim. Biophys. Acta* **1980**, *631*, 232−245.
(43) van Niekerk, J. N.; Schoening, F. R. L. *Acta Crystallogr.* **1953**, *6*, 227−232.
(44) de Meester, P.; Fletcher, S. R.; Skapski, A. C. *J. Chem. Soc., Dalton Trans.* **1973**, 2575−2578.
(45) Brown, G. M.; Chidambaram, R. *Acta Crystallogr., Sect. B* **1973**, *B29*, 2393−2403.
(46) Wilkinson, G. *Comprehensive Coordination Chemistry. The Synthesis, Reaction, Properties & Application of Coordination Compounds*; Pergamon Press: Oxford, 1987; Vol. 5, pp 634−774.

Table 3. Lattice Parameters and Selected Details of Refinements of the Powder Diffraction Patterns of $[Cu_2(Indo)_4(L)_2]$ Complexes

params	$[Cu_2(Indo)_4(DMF)_2]$	$[Cu_2(Indo)_4(OH_2)_2]\cdot 1.5H_2O$	$[Cu_2(Indo)_4(NMP)_2]$	$[Cu_2(Indo)_4(DMA)_2]$
a (Å)	10.850(7)	11.17(3)	22.104(6)	11.10(2)
b (Å)	13.360(7)	14.84(4)	25.941(9)	12.98(2)
c (Å)	16.56(1)	16.26(7)	15.375(7)	15.97(12)
α (deg)	105.8(1)	103.1(3)	91.80(3)	100.7(3)
β (deg)	101.1(1)	104.8 (3)	107.17(3)	101.2(3)
γ (deg)	106.9(1)	100.0(3)	108.48(4)	109.7(2)
	triclinic	triclinic	triclinic	triclinic

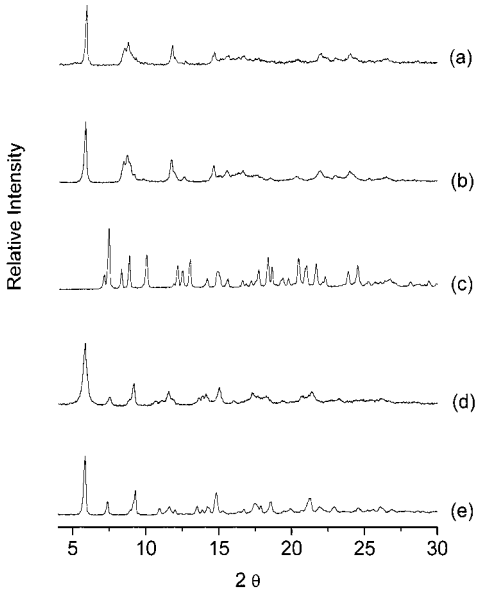

Figure 3. X-ray powder diffraction patterns of (a) $[Cu_2(Indo)_4(OH_2)_2]$, (b) $[Cu_2(Indo)_4(OH_2)_2]\cdot 1.5H_2O$, (c) $[Cu_2(Indo)_4(NMP)_2]$, (d) $[Cu_2(Indo)_4(DMA)_2]$, and (e) $[Cu_2(Indo)_4(DMF)_2]$.

Cu carboxylate dimers[23−26] and only slightly longer than that found in Cu metal (2.56 Å).[47]

X-ray Powder Diffraction Patterns. The powder patterns of all of the complexes were indexed as having a triclinic cell with lattice parameters given in Table 3. X-ray powder diffraction patterns for $[Cu_2(Indo)_4(DMF)_2]$, $[Cu_2(Indo)_4(DMA)_2]$, $[Cu_2(Indo)_4(NMP)_2]$, $[Cu_2(Indo)_4(OH_2)_2]\cdot 1.5H_2O$ and $[Cu_2(Indo)_4(OH_2)_2]$ are shown in Figure 3.

With the exception of the $[Cu_2(Indo)_4(OH_2)_2]$ complex, the microcrystalline samples were reasonably crystalline and gave well-resolved X-ray diffraction patterns over the range $2° < 2\theta < 35°$. The small number of well-resolved lines observed in the diffraction pattern of $[Cu_2(Indo)_4(OH_2)_2]$ prevented indexing of this pattern. X-ray diffraction patterns for the other complexes could only be indexed on the basis of a triclinic cell. The cell dimensions of the DMF complex are similar to those obtained from the single-crystal measurements; the small differences probably arose from different DMF/H_2O solvents of crystallization in the two samples. The cell dimensions of the DMF complex are also similar to those of the DMSO complex.[42] Figure 3 clearly shows that the $[Cu_2(Indo)_4(OH_2)_2]$ and $[Cu_2(Indo)_4(OH_2)_2]\cdot 1.5H_2O$ complexes are isostructural, and the DMF and DMA complexes are isostructural. It is clear that these two pairs of compounds are not isostructural with each other, as is evident from the strong 002 reflection near 7.5° in the DMF and DMA complexes.

The diffraction pattern of the NMP complex is unique when compared to those observed for either the DMF/DMA or the $H_2O/[Cu_2(Indo)_4(OH_2)_2]\cdot 1.5H_2O$ complexes. For the NMP complex, there appears to be a doubling of both the a and b cell dimensions, while c remains unchanged, when compared to the DMF complex. No clear relationship, however, is observed between the a, b, and c cell dimensions for the NMP complex when compared to the unit cells of the other complexes.

UV−Vis and IR Spectroscopies. The diffuse reflectance UV−vis spectra of (a) IndoH, (b) $[Cu_2(Indo)_4(DMF)_2]$, and (c) Cu(II) acetate monohydrate in a KBr matrix and solid state IR spectra of (a) $[Cu_2(Indo)_4(DMF)_2]$ and (b) IndoH in a KBr matrix are provided as Supporting Information. The solid and solution state electronic spectra of all of the $[Cu_2(Indo)_4L_2]$ complexes show a broad absorption band (band I) in the visible region around 700 nm (Table 4), which is assigned to a $d_{xy,yz} \rightarrow d_{x^2-y^2}$ transition.[25,31,48] There is a slight shoulder around 790 nm, which is typical of a Jahn−Teller-distorted Cu(II). This is similar to that reported for $[Cu_2(Indo)_4(DMSO)_2]$.[42] The solid state spectra all display a shoulder at ∼330 nm (band II). The origin of band II remains unclear but has been assigned to a charge-transfer absorption.[49] Band II is believed to be indicative of a dimeric complex[23,30,50] even though a number of monomeric and polymeric Cu(II) compounds exhibit this band.[49,51,52] All of the complexes, however, display bands I and II in the usual range for Cu(II) compounds in a square-pyramidal CuO_4O environment.[46,53] None of the solid state spectra display a carboxy−copper(II) charge-transfer absorption in the 240−280-nm range (band III),[54] because IndoH has a strong absorption in the 200−400-nm range. Consequently, band II of the Cu complexes partially overlaps with this band and band III is concealed. The diffuse reflectance spectra of the $[Cu_2(Indo)_4L_2]$ complexes do, however, show a small shoulder at 300−330 nm (Table 4) and possibly a second small absorption band at 240−280 nm. The shoulder at 300−330 nm is similar to those displayed in Cu(II) acetate monohydrate, Cu(II) cyanoacetate, and Cu(II) cyanoacetate monohydrate[55] and may be due to band II. The assignment of the shoulder near 260 nm (band III) is less certain.

Since the intensity of band I can be appreciably higher for dinuclear carboxylate complexes[22,23,25,28,56−58] than for mononuclear complexes, it has been suggested that this is diagnostic.[22,23] However, the molar absorptivities for the monomeric

(47) Aylward, G. H.; Findlay, T. J. V. *SI Chemical Data*, 2nd ed.; John Wiley & Sons Australasia Pty. Ltd.: New York, 1971.
(48) Kato, M.; Muto, Y. *Coord. Chem. Rev.* **1988**, *92*, 45−83.
(49) Catterick, J.; Thornton, P. *Adv. Inorg. Chem. Radiochem.* **1977**, 291−362.
(50) Dubicki, L.; Martin, R. L. *Inorg. Chem.* **1966**, *5*, 2203−2209.
(51) Hathaway, B. J.; Billing, D. E. *Coord. Chem. Rev.* **1970**, *5*, 143−207.
(52) Yawney, D. B. W.; Moreland, J. A.; Doedens, R. J. *J. Am. Chem. Soc.* **1973**, *95*, 1164−1170.
(53) Agterberg, F. P. W.; Provo Kluit, H. A. J.; Driessen, W. L.; Reedijk, J.; Oevering, J.; Buijs, W.; Veldman, N.; Lakin, M. T.; Spek, A. L. *Inorg. Chim. Acta* **1998**, *267*, 183−192.
(54) Graddon, D. P. *J. Inorg. Nucl. Chem.* **1961**, *17*, 222−231.
(55) Wasson, J. R.; Shyr, C.-I.; Trapp, C. *Inorg. Chem.* **1968**, *7*, 469−474.
(56) Ahmed, I. Y.; Abuhijleh, A. L. *Inorg. Chim. Acta* **1982**, *61*, 241−246.
(57) Abuhijleh, A. L.; Woods, C. *Inorg. Chim. Acta* **1993**, *209*, 187−193.
(58) Kokot, E.; Martin, R. L. *Inorg. Chem.* **1964**, *3*, 1306−1312.

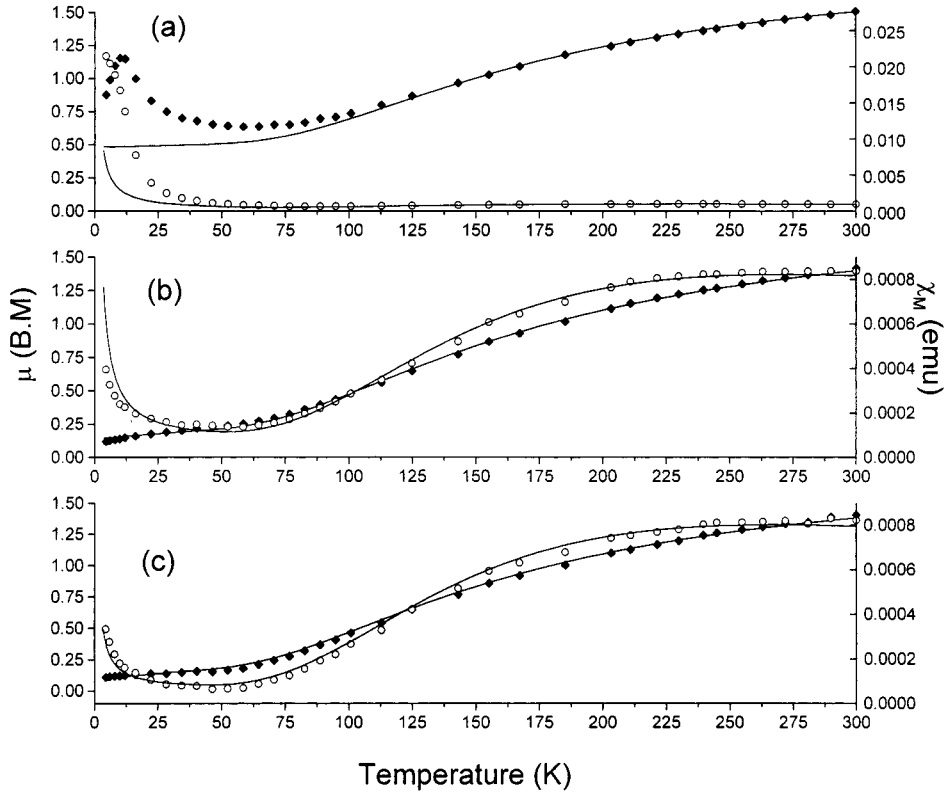

Figure 4. Plots of χ_M (○, observed; —, calculated) and μ (◆, observed; —, calculated) versus T for (a) $[Cu_2(Indo)_4(OH_2)_2]$, (b) $[Cu_2(Indo)_4(DMF)_2]$, and (c) $[Cu_2(Indo)_4(OH_2)_2]\cdot 1.5H_2O$.

Table 4. Room Temperature Magnetic Moments, SQUID Variable Temperature Magnetic Data, and Electronic Absorption Spectral Data for the $[Cu_2(Indo)_4(L)_2]$ Complexes

compd	μ_{eff}[a,b] (T = 300 K)	g value[b]	J (cm^{-1})[b]	N_α (cgs)[b]	fraction[b] monomer	ν_{asym}(COO) (cm^{-1})	ν_{Cu-O} (cm^{-1})	λ_{max} (nm)[c] (ϵ_{max} (M^{-1} cm^{-1}))
$[Cu_2(Indo)_4(DMF)_2]$	1.42	2.10	−152.5(1)	0.000 06	0.006	1618 s	363 s, 321 s	709 s (417), 326 sh
$[Cu_2(Indo)_4(OH_2)_2]\cdot 1.5H_2O$	1.40	2.06	−149.8(1)	0.000 06	0.002	1630 s	385 s, 331 s	708 s (460), 327 sh
$[Cu_2(Indo)_4(DMA)_2]$	1.52	2.16	−142.3(1)	0.000 06	0.09	1599 s	382 s, 319 s	709 s (395), 329 sh
$[Cu_2(Indo)_4(NMP)_2]$	1.53	2.25	−142.3(1)	0.000 06	0.01	1622 s	388 s, 340 s	709 s (441), 319 sh
$[Cu_2(Indo)_4(OH_2)_2]$	1.51	2.17	−144(1)	0.000 06	0.065	1630 s	386 s, 332 s	709 s (450), 324 sh
$[Cu_2(CH_3COO)_4(OH_2)_2]$	1.53[d]	2.1	−142(1)	0.000 06[b]		1618 s	376 s, 331 s	703 s (191), 355 sh

[a] Calculated using monomeric formula weight. [b] Derived from variable temperature magnetic susceptibility data. [c] s = strong; sh = shoulder. [d] Taken from ref 68.

pyridine analogue of the Cu complexes of the NSAIDs naprosyn, ϵ_{dmf} = 301 M^{-1} cm^{-1}, and ibuprofen, ϵ_{dmf} = 263 M^{-1} cm^{-1},[25] are similar to that of a dimeric DMSO Cu(II) complex of ibuprofen, ϵ_{dmf} = 398 M^{-1} cm^{-1}.[25] Furthermore, the reported value of the molar absorptivity for the dimeric DMSO Cu(II) complex of ibuprofen (ϵ = 178 M^{-1} cm^{-1})[24] is approximately half that for the dimeric $[Cu_2(Indo)_4(L)_2]$ complexes under investigation ($\epsilon \approx$ 349 M^{-1} cm^{-1}). Thus it is clear that the intensity of band I cannot be used to definitively determine the presence of monomeric or dimeric units.

In principle, the mode of coordination of the carboxylate to the central Cu ion can be determined from the value of Δ ($\Delta = \nu_{asym} - \nu_{sym}$)[59−61] in the IR spectra. This criterion could not be used in the present $[Cu_2(Indo)_4L_2]$ complexes, since the carboxylate stretching frequencies are obscured by other bands (Supporting Information). The Cu−O stretching frequencies (Table 4) are comparable to those reported for Cu(II) acetate type dimers.[62−64]

UV−vis and IR spectroscopies, together with elemental analysis, of the $[Cu_2(Indo)_4L_2]$ complexes are suggestive, rather than definitive, of a dimeric Jahn−Teller-distorted Cu site. Thus, magnetic susceptibility and EPR measurements were undertaken to determine both the nature and extent of any Cu−Cu interactions in the complexes.

Magnetic Susceptibility. The room temperature magnetic moments per Cu (μ_{eff} = 1.40−1.56 μ_B, Table 4) are similar to those observed for other dinuclear Cu(II) compounds of the type $[Cu_2(RCOO)_4L_2]$[65,66] and are lower than the d^9 spin-only magnetic moment, μ_{eff} = 1.73 μ_B. This observation is consistent with antiferromagnetic exchange between the two Cu(II) ions.[32,67] The variable temperature magnetic results for $[Cu_2(Indo)_4(OH_2)_2]$, $[Cu_2(Indo)_4(DMF)_2]$, and $[Cu_2(Indo)_4(OH_2)_2]\cdot$

(59) Deacon, G. B.; Phillips, R. J. *Coord. Chem. Rev.* **1980**, *33*, 227−250.
(60) Nakamoto, K. *Infrared Spectra of Inorganic and Organometallic Compounds*; Wiley: New York, 1963.
(61) Tyagi, A. S.; Srivastava, C. P. *J. Indian Chem. Soc.* **1981**, *58*, 284−286.
(62) Faniran, J. A.; Patel, K. S. *J. Inorg. Nucl. Chem.* **1974**, *36*, 2261−2263.
(63) Mathey, Y.; Greig, D. R.; Shriver, D. F. *Inorg. Chem.* **1982**, *21*, 3409−3413.
(64) Fanisan, J. A.; Patel, K. S. *J. Inorg. Nucl. Chem.* **1979**, *41*, 1495−1496.
(65) Casanova, J.; Alzuet, G.; LaTorre, J.; Borras, J. *Inorg. Chem.* **1997**, *36*, 2052−2058.
(66) Doedens, R. J. *Prog. Inorg. Chem.* **1976**, *21*, 209−231.
(67) Figgis, B. N.; Martin, R. L. *J. Chem. Soc.* **1956**, 3837−3846.

Table 5. X-Band and Zero-Field EPR Data for the $[Cu_2(Indo)_4(L)_2]$ Complexes

sample	T (K)	g values[a] (110 K)	D (GHz) (10^{-2} cm^{-1})[b]	coordination	E (GHz) (cm^{-1})[b]	$A_{\|\|}$ (MHz) (10^4 cm^{-1})[b]
$[Cu_2(Indo)_4(H_2O)_2]$[d]	90	$g_{\|\|}$ 2.35, $g_\perp$ 2.05, g_{eff} 2.15[c]	9.975(1) (33.273(3))	CuO_5	0.028(2) (9.3(6) × 10^{-4})	230.5(2) (76.88(7))
$[Cu_2(Indo)_4(OH_2)]\cdot 1.5H_2O$[d]	120	$g_{\|\|}$ 2.35, $g_\perp$ 2.05, g_{eff} 2.15[c]	10.003(1) (33.366(3))	CuO_5	0.017(3) (5.7(9) × 10^{-4})	229.0(5) (75.4(2))
$[Cu_2(Indo)_4(DMF)_2]$[d]	90	$g_{\|\|}$ 2.36, $g_\perp$ 2.06, g_{eff} 2.16[c]	10.217(1) (34.080(3))	CuO_5	0.051(2) (1.70(6) × 10^{-3})	230.0(5) (76.7(2))
$[Cu_2(Indo)_4(NMP)_2]$[d]	145	$g_{\|\|}$ 2.36, $g_\perp$ 2.06, g_{eff} 2.16[c]	10.317(1) (34.414(3))	CuO_5	0.085(1) (2.84(3) × 10^{-3})	219.2(5) (73.1(2))
$[Cu_2(CH_3COO)_4(OH_2)_2]$		$g_{\|\|}$ 2.42, $g_\perp$ 2.08, g_{eff} 2.19[f]	10.08(2)[e] (33.623(6))	CuO_5	0.296[e] (0.01 ± 0.005)[f]	

[a] g value derived from X-band simulations; for an anisotropic system: $g_{\|\|} = g_z$, and $g_\perp = g_{xy}$. [b] D, E, and $A_{\|\|}$ derived from ZFEPR simulations. [c] $g_{eff} = (1/3)(g_{\|\|} + 2g_\perp)$. [d] Sample contained traces of monomer. [e] Taken from ref 35. [f] Taken from ref 32.

$1.5H_2O$ are plotted in Figure 4, panels a, b, and c, respectively, along with the lines of best fit, and the calculated values of J are given in Table 4 for all of the $[Cu_2(Indo)_4(L)_2]$ complexes.

The magnetic moments of the Cu−Indo complexes decrease from around 1.50 μ_B at 300 K to approximately 0.2 μ_B at 4.5 K, as a consequence of depopulation of the excited triplet ($S = 1$) state.[58,67,68] The susceptibilities display a maximum at approximately 300 K and decrease to a minimum value near 50 K. Below this, there is a rapid increase in magnetic susceptibility as the temperature is lowered further to 4.5 K. The behavior below 50 K is a consequence of a small amount (≤1%, Table 4) of a monomeric Cu(II) ion.

The temperature dependence of the magnetic properties of $[Cu_2(Indo)_4(OH_2)_2]$ was significantly different. The magnetic moment decreased with decreasing temperature from 1.51 μ_B at 300 K to 0.63 μ_B at 50 K in a manner similar to that observed for the other dimers. At temperatures below 50 K, the value of μ_{eff} initially increases with decreasing temperature, reaching a maximum of 1.5 μ_B at 10 K, and then it decreases again to ~0.88 μ_B at 4.5 K. This increase in magnetic moment with decreasing temperature from 50 to 10 K is unusual and is suggestive either of interdimer ferromagnetic coupling, perhaps via some hydrogen-bonding interaction involving the water molecules, or of a magnetic impurity.

Zero-Field EPR Spectroscopy. ZFEPR spectra were measured for all of the complexes at 90, 120, and 145 K to determine values for D and E, prior to simulation of the X-band EPR spectra. Despite the atypical magnetic susceptibilities of $[Cu_2(Indo)_4(OH_2)_2]$ below 50 K, the magnetic properties for all of the complexes studied were similar at the temperatures relevant to the EPR studies. The results of the least-squares refinements for the values of D, E, g, and $A_{\|\|}$ are set out in Table 5.

As illustrated for $[Cu_2(Indo)_4(OH_2)_2]$ in Figure 5, the complexes exhibit 7-line ZFEPR spectra centered near 10 GHz. In all cases, the inner peaks were of comparable intensity. The D and g parameters are typical of those for octahedral Cu(II) carboxylate complexes where the unpaired electron is in a $d_{x^2-y^2}$ orbital.[69,70] The observed D values, 0.333 and 0.344 cm^{-1}, are comparable to those found for dinuclear Cu compounds with exclusively oxygen donors ($D = 0.34$ cm^{-1}).[71,72] The best-fit E values are all very small, in keeping with the strong axial symmetry observed in related X-band spectra.

X-Band EPR Powder Spectra. Typical powder spectra for the $[Cu_2(Indo)_4L_2]$ complexes are shown in Figure 6, and the best-fit parameters are summarized in Table 5. The line shape and peak positions of the spectra were not substantially influenced by the axial ligands. All spectra exhibited features typical of those for dimeric complexes with axial symmetry and $g_{\|\|} > g_\perp$[66,69,73] and a $d_{x^2-y^2}$ (or d_{xy}) ground state.[46] The spectra are better resolved than that of $[Cu_2(Indo)_4(DMSO)_2]$ described by Weser,[42] and in all cases they exhibit, at room temperature, a broad resonance at $g_{eff} \approx 2.1$ ($H_{\perp 2} \approx 4720$ G), with weak features at ~5980 (H_{z2}) and 500 G (H_{z1}) due to the spin-triplet state of the dimeric complex and a small resonance at 3300 G due to a Cu(II) monomer impurity. On cooling to 110 K, the

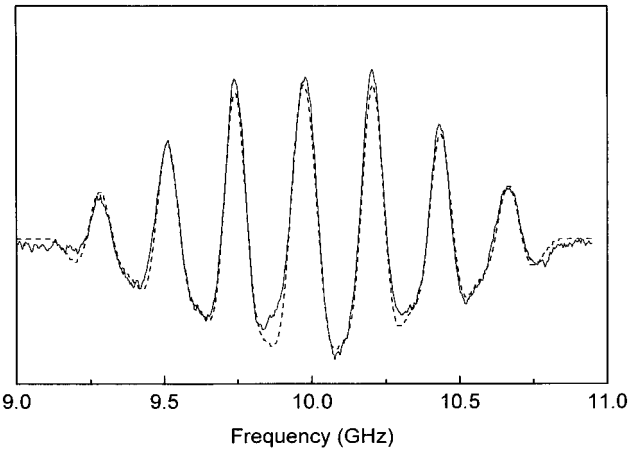

Figure 5. Experimental (solid line) and calculated (dashed line) ZFEPR spectra of $[Cu_2(Indo)_4(OH_2)_2]$, $T = 90$ K, $B_\pm = 2$ mT.

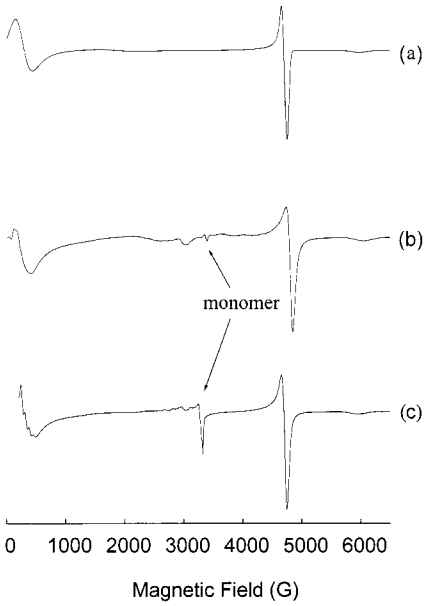

Figure 6. $[Cu_2(Indo)_4(DMF)_2]$ X-band powder EPR spectra: (a) simulation of 110 K spectrum; (b) 295 K; (c) 110 K.

(68) Hadjikostas, C. C.; Katsoulos, G. A.; Sigalas, M. P.; Tsipis, C. A.; Mrozinski, J. *Inorg. Chim. Acta* **1990**, *167*, 165−169.
(69) Melnik, M. *Coord. Chem. Rev.* **1981**, *36*, 1−44.
(70) Smith, T. D.; Pilbrow, J. R. *Coord. Chem. Rev.* **1974**, *13*, 173−278.
(71) Goodgame, D. M. L.; Nishida, Y.; Winpenny, R. E. P. *Bull. Chem. Soc. Jpn.* **1986**, *59*, 344−346.
(72) Price, J. H.; Pilbrow, J. R.; Murray, K. S.; Smith, T. D. *J. Chem. Soc. A* **1970**, 968−976.
(73) Mabbs, F. E. *Chem. Soc. Rev.* **1993**, *22*, 313−324.

broad resonance at $g_{eff} = 2.1$ decreases in intensity, with a corresponding increase in amplitude of the features due to the triplet state. At 110 K, the monomer feature becomes more evident and the powder spectrum exhibits a distinctive absorption at 3300 G. Calculated values of the monomeric fraction for the complexes studied, as derived from the variable temperature magnetic susceptibility data, are given in Table 4.

The average values for g for the complexes studied are in good agreement with those obtained from variable temperature magnetic susceptibility measurements. In addition, both the $g_{\|}$ and $g_{\perp}$ values for the $[Cu_2(Indo)_4L_2]$ complexes are similar to those reported for other dinuclear Cu(II) carboxylate adducts,[66,69,74] where $g_{\|} \approx 2.3$, $g_{\perp} \approx 2.08$, and $D \approx 0.34$ cm^{-1},[75] and for Cu(II)−Indo and its water[76] and DMSO adducts.[42]

Previous workers have proposed that the value of $g_{\|}$ is indicative of an axial environment, with oxygen donors given a lower value of $g_{\|}$ compared to nitrogen donors.[28] The finding of equivalent values of $g_{\|}$ for the complexes studied is, therefore, suggestive of equivalent symmetry around the Cu ion and similar ligand fields due to the various adducts.

Solution Studies. When $[Cu_2(Indo)_4(DMF)_2]$ was dissolved as a micellar solution in HEPES and TES, the UV−vis spectra remained characteristic of the Cu(II) dimer over a 3 day period, with little change in either the Cu absorbance at 709 nm or the indomethacin absorbance at 325 nm. In addition, EPR spectroscopy indicated that <8% of Cu(II) monomer was present. Likewise, the Span 80 plus tetraglycol micellar solution indicated <1% of Cu(II) monomer present.

Discussion

Four Cu(II) dimers of Indo have been prepared and characterized. The analytical data and physical measurements are consistent with the dimeric structures of the $[Cu_2(Indo)_4L_2]$ complexes.

Structures of Cu Indomethacin in Relation to Pharmaceutical Activity. The $[Cu_2(Indo)_4(L)_2]$ complexes act as effective anti-inflammatory drugs in dogs without leading to gastrointestinal bleeding and death.[26,77] This indicates that Indo is not released from Cu^{2+} during ingestion via the gastrointestinal tract, since IndoH itself cannot be used as an anti-inflammatory drug for dogs because of these fatal side effects.[78−80]

To understand the pharmacology of these drugs and, hence, their potential for use as human pharmaceutical agents, it is important to understand the properties of the complexes in terms of their stabilities and structures. In particular, it was important to assess whether the terminal ligands had any effects on the structures and properties of the complexes, since a variety of pharmaceutical preparations have been used in which different solvent molecules are coordinated to the Cu^{2+} center, in addition to Indo.

The results of the spectroscopic and magnetic measurements establish that a dinuclear Cu acetate-type structure is maintained for all of the complexes. The X-ray structure of the DMF complex not only confirmed this but also provided some important clues as to the features of the drugs that may be important in their pharmacology. The DMF complex has no significant intermolecular contacts in the unit cell. This hydrophobic molecule is contained in micelles in some pharmaceutical preparations and biological buffer solutions, and a hydrophobic environment of the micelles would help prevent the decomposition of the dinuclear species. EPR and UV−vis spectroscopies of the micelle and buffer solutions of the DMF complex confirm that the complex remains intact in the dinuclear form; however, lack of sensitivity of these techniques to the nature of the axial ligand does not allow changes in the axial ligation to be determined. The hydrophobic nature of these complexes is also likely to be important in allowing the transport of the drug, in an intact form, through the biological membranes of the gastrointestinal tract and hence, minimization of the adverse biological effects of free IndoH in the gastrointestinal tract.

Copper−Copper Interactions in the Dinuclear Complexes. The large negative J values obtained from the variable temperature magnetic susceptibility studies (Table 4) show that the $[Cu_2(Indo)_4(L)_2]$ complexes have a singlet ground state with a triplet excited state, which is 284−304 cm^{-1} ($2J$) higher in energy. The observed values of J are comparable to those of other dinuclear Cu(II) complexes,[49,68] including Cu(II) acetate monohydrate ($J = -142$ cm^{-1}).[49] Dimeric Cu(II) arylcarboxylates have a stronger coupling, J values around -150 cm^{-1}, compared to polymeric materials, $J \approx 50$ cm^{-1},[66,68,81] further confirming the dimeric nature of the present complexes.

While the fine details remain obscure, it is clear that dinuclear compounds with either a CuO_4N or CuO_5 coordination have noticeably different average values, of $-2J = 348$ and 316 cm^{-1}, respectively.[74] This observation is consistent with the results for $[Cu_2(Indo)_4(H_2O)_2]$, $[Cu_2(Indo)_4(NMP)_2]$, and $[Cu_2(Indo)_4(DMF)_2]$, where the average value of $-2J$ is 294 cm^{-1}.[82] The strength of the antiferromagnetic coupling was independent of the nature of the axial ligand. Conflicting evidence exists in the literature concerning the influence of the nature of the terminal ligand on the value of J. Some workers have proposed that the value of J is only weakly dependent on the nature of the axial donor ligand and is not a simple function of the base strength of the bridging carboxylate ligand,[66] whereas others have concluded that the strength of the antiferromagnetic interaction tends to increase as either the axial ligand, L, or the carboxylate constituent becomes a stronger electron donor,[83] and the pK_a value of L increases.[84,85] In addition, larger J values have been attributed to a weaker σ donation by the axial ligand, with the suggestion that when there is a corresponding increase in the ligand field of the four carboxylato oxygen atoms around the metal ion, larger splitting of the d−d energy levels and a blue shift of band I result.[48,50] It is, however, well established that the magnitude of the magnetic coupling is sensitive to the Cu−O−C−O−Cu geometry,[69] and the similarity in J and λ_{max} among the complexes suggests that they all retain a similar Cu_2O_8 core.[53,74]

(74) Melnik, M. *Coord. Chem. Rev.* **1982**, *42*, 259−293.
(75) Bencini, A.; Gatteschi, D. *EPR of Exchange Coupled Systems*; Springer-Verlag: Berlin, 1990.
(76) David, L.; Cosar, O.; Chis, V.; Negoescu, A.; Vlasin, I. *Appl. Magn. Reson.* **1994**, *6*, 521−528.
(77) *IVS Annual*; MIMS Publishing: Crows Nest, NSW, Sydney, 1997; pp 145, 276.
(78) Adams, H. R. *Veterinary Pharamacology and Therapeutics*, 7th ed.; Iowa State University Press: Ames, IA, 1995; pp 443−444.
(79) Ewing, G. O. *J. Am. Vet. Med. Assoc.* **1972**, *161*, 1665−1668.
(80) Menguy, R.; Desbaillets, L. *Am. J. Dig. Dis.* **1967**, *12*, 862−866.
(81) Herring, F. G.; Landa, B.; Thomson, R. C.; Schewdtfeger, C. F. *J. Chem. Soc. A.* **1971**, 528−535.
(82) The unusual magnetic properties are not due to trapped oxygen. This was confirmed by low-temperature magnetism studies, where O_2 has characteristic behavior. Furthermore, the EPR studies do not show any triplet signals due to O_2. Although several attempts have been made at growing crystals of the aqua complex, we are yet to obtain crystals suitable for XRD analysis.
(83) Jotham, R. W.; Kettle, S. F. A.; Marks, J. A. *J. Chem. Soc., Dalton Trans.* **1972**, 428−438.
(84) Marsh, W. E.; Carlisle, G. O.; Hanson, M. V. *J. Mol. Struct.* **1977**, *40*, 153−156.
(85) Marsh, W. E.; Carlisle, G. O.; Hanson, M. V. *J. Inorg. Nucl. Chem.* **1977**, *39*, 1839−1841.

The only measurable difference found among all the complexes is in the value of *D*, as measured by ZFEPR, with the DMF and NMP ligands contributing to a greater extent to the exchange between the ground state of one Cu and the excited state of the other Cu, compared to the water ligand.

The magnitude of the axial splitting, *D*, is a function of two terms:[70,72,86,87] a dipolar contribution D^{dip}, which is related to the Cu−Cu distance, and the exchange contribution, D^{exch}. The latter term is more critical, for complexes with weaker-field donors that have excited states nearer in energy to the ground state, so yielding large values of D^{exch} and hence *D*. Conversely, for a strong-field donor, the energy gap to the excited state is larger, leading to a smaller value for D^{exch} and, hence, *D*.

Assuming that the Cu−Cu separation and, hence, D^{dip} are comparable for the various complexes under investigation, it would appear that the $[Cu_2(Indo)_4(DMF)_2]$ and $[Cu_2(Indo)_4(NMP)_2]$ complexes have a weaker ligand-field contribution from their respective axial ligands (as indicated by a higher value for *D*) when compared to those of the water complexes. These very small differences in the value of *D* do not influence either the UV−vis spectra (the energies of band I and band II are not sensitive indicators to small differences in bonding) or the strength of the antiferromagnetic exchange (*J*).

The important conclusion that flows from the electronic and magnetic studies of the complexes is their relative insensitivity to changes in the axial ligands. Since the axial ligands are likely to exchange during drug metabolism, these results show that the physical properties and, hence, reactivities and efficacies of the drug are likely to be insensitive to the nature of the axial ligands. This is consistent with the lack of variation in the pharmaceutical activities of the Cu−Indo drugs with different axial ligands.[26,88]

In addition, the other important aspect of the magnetic and EPR measurements is that they are extremely sensitive to mononuclear Cu^{2+} at low temperatures as a result of the diamagnetic ground states of the dinuclear species. Thus, both techniques are valuable in quality control of pharmaceutical preparations, since even small amounts of mononuclear Cu^{2+} can be quantified readily by such techniques. EPR spectroscopy, however, is a more convenient technique for this application. The results reported here establish that the concentrations of such impurities are very low (<1%) in the complexes used for pharmaceutical preparations.

Acknowledgment. We acknowledge the support of this work by the University of Sydney Major Equipment fund and an Australian Research Council (ARC) RIEFP grant for the EPR spectrometers, an ARC Large grant to Monash University (K.S.M.), an ARC SPIRT grant (P.A.L., T.W.H., B.J.K., J.R.B., H.L.R.), and Biomedical Veterinary Research (BVR) for the funding of a postgraduate scholarship for J.E.W. We also thank Dr. Bradley Collins and Mr. Alan MacKenzie for useful suggestions in the course of the IR study and Prowski refinements, respectively.

Supporting Information Available: Tables of non-hydrogen positional parameters, bond distances, bond angles, anisotropic thermal parameters, and hydrogen atom positions and isotropic thermal parameters for $[Cu_2(Indo)_4(DMF)_2]$, tables of observed and calculated variable temperature magnetic susceptibility and magnetic moment values per Cu ion in emu and μ_B units, respectively, for $[Cu_2(Indo)_4(DMF)_2]$, $[Cu_2(Indo)_4(NMP)_2]$, $[Cu_2(Indo)_4(OH_2)_2]\cdot 1.5H_2O$ and $[Cu_2(Indo)_4(OH_2)_2]$, figure of the diffuse reflectance UV−vis spectra of (a) IndoH, (b) $[Cu_2(Indo)_4(DMF)_2]$, and (c) Cu(II) acetate monohydrate in a KBr matrix, figure of the solid state IR spectra of (a) $[Cu_2(Indo)_4(DMF)_2]$ and (b) IndoH in a KBr matrix, and figures of the atomic numbering system for Indo attached to C_{21} and C_1* in the crystal structure of $[Cu_2(Indo)_4(DMF)_2]$. This material is available free of charge via the Internet at http://pubs.acs.org.

IC981100X

(86) Mabbs, F. E.; Collison, D. *Electron Paramagnetic Resonance of d Transition Metal Compounds*; Elsevier: Amsterdam, 1992.

(87) Blake, A. J.; Grant, C. M.; McInnes, E. J. L.; Mabbs, F. E.; Milne, P. E. Y.; Parsons, S.; Rawson, J. M.; Winpenny, R. E. P. *J. Chem. Soc., Dalton Trans.* **1996**, *21*, 4077−4082.

(88) Regtop, H. L.; Biffin, J. R. Divalent Metal Complexes of Indomethacin, Compositions and Medical Methods of Use Thereof. US Patent 5466824; Biochemical Veterinary Research Pty. Ltd., Australia, 1995.